

# Preparation of TiO<sub>2</sub> Nanoparticles/2,2'-(1,3-propanediylbisnitrilo-ethylidene)bis-Hydroquinone Carbon Paste Electrode and Its Application for Simultaneous Sensing of Trace Amounts of Ascorbic acid, Uric acid and Folic acid

Mohammad Mazloun-Ardakani<sup>1,\*</sup>, Rezvan Arazi<sup>1</sup>, Hossein Naeimi<sup>2</sup>

<sup>1</sup>Department of Chemistry, Faculty of Science, Yazd University, Yazd, 89195-741, I. R. Iran

<sup>2</sup>Department of Organic Chemistry, Faculty of Chemistry, University of Kashan, Kashan, 87317, I.R.Iran

\*E-mail: [mazloun@yazduni.ac.ir](mailto:mazloun@yazduni.ac.ir)

Received: 28 May 2010 / Accepted: 15 October 2010 / Published: 1 December 2010

---

A carbon paste electrode modified with 2,2'-(1,3-propanediylbisnitrilo-ethylidene)bis-hydroquinone (PBNBH) and TiO<sub>2</sub> nanoparticles was prepared. The modified carbon paste electrode exhibits excellent electrocatalytic activity towards the oxidation of ascorbic acid (AA), uric acid (UA) and folic acid (FA) and reduced the overpotential for AA oxidation to about 380 mV lower than that of the bare electrode. The modified carbon paste electrode could separate the anodic peaks of AA, UA and FA in a mixture. Potential differences of 330 mV (AA/UA) and 560 mV (AA/FA) were observed, which were large enough to allow for the determination of AA, UA and FA. The catalytic peak current obtained from differential pulse voltammetry (DPV) was linearly dependent on the AA concentration in the range of 4.0-600.0 μM. The detection limit (2σ) for AA was 0.4 μM with a sensitivity of 0.785 μA μM<sup>-1</sup> and a correlation coefficient of 0.9998. The electron transfer rate constant,  $k_s$ , and charge transfer coefficient,  $\alpha$ , were calculated to be 1.55 s<sup>-1</sup> and 0.34, respectively.

---

**Keywords:** Carbon paste electrode, TiO<sub>2</sub> nanoparticles, Ascorbic acid, Uric acid, Folic acid

## 1. INTRODUCTION

Numerous studies have focused on the properties of nanoparticles in electrochemistry and heterogeneous catalysis, partially because of their importance in the design of practical gas diffusion electrodes and catalysts. The influence of the size and surface structure of nanoparticles on their electrocatalytic and catalytic properties has also been the aim of several works. Due to its unique physical chemistry properties [1–3] and the physiochemical inclination to selectively combine with some groups of biomolecules, TiO<sub>2</sub> nanoparticles (nano-TiO<sub>2</sub>) are an attractive, biocompatible and

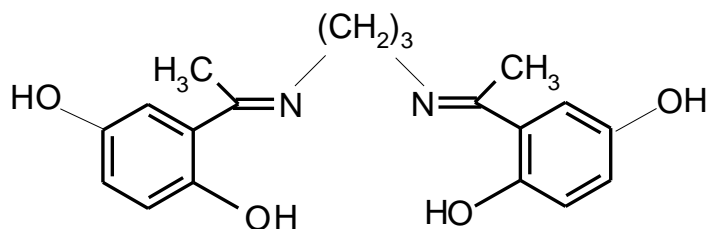
environmentally benign material widely used in toothpaste and cosmetics. In contrast to its broad application in photochemistry [4–6], there are few studies of nano-TiO<sub>2</sub> electrochemistry. The major barriers involve the low solubility and poor stability of TiO<sub>2</sub> nanoparticles and the TiO<sub>2</sub> film on the electrodes.

Ascorbic acid (AA) or vitamin C is distributed widely in both the plant and animal kingdoms. In vegetable cells, it exists in its free form and also often binds to several proteins, such as ascorbigen. Among animal organs, the liver, leukocytes and anterior pituitary lobe contain the highest concentrations of ascorbic acid. Vitamin C is also present in many other biological systems and multivitamin preparations, which are commonly used to supplement inadequate dietary intake. It is widely used in foods as an antioxidant for the stabilization of color and aroma for extension of their storage time [7–9]. By contrast, uric acid (UA) is the primary product of purine metabolism in humans. Extreme abnormalities of UA levels are symptoms of several diseases, such as gout, hyperuricemia and Lesch–Nyhan syndrome [10, 11]. Therefore, it is essential to develop simple and rapid methods for determination of these biological molecules for routine analysis. However, the direct determination of AA at ordinary (carbon or metal) electrodes is challenging, because of the large overpotential of AA and fouling by oxidation products [12]. Moreover, at bare electrodes, the oxidation of UA, which is always present with AA in biological tissues, occurs at a potential close to that of AA. Therefore, it is essential to separate the oxidation potentials of AA and UA from each other. Similarly, folic acid (FA) is an important component of the hematopoietic system and is the coenzyme that controls the generation of ferroheme [13]. Lack of FA gives rise to gigantocytic anemia and is associated with leucopenia, devolution of mentality and psychosis. Determination of FA is often required in pharmaceutical, clinical and food samples.

To overcome the problems of selectivity, the electrode surface can be modified to decrease the overpotential, improve the mass transfer velocity and effectively enrich the substance [14, 15]. Surface modification of electrodes is one of the most exciting developments in the field of electroanalytical chemistry. Modification may lead to significant reduction of overpotentials and increased electron transfer rate constants of the desired redox reactions at the electrode for electrochemically selective and sensitive determination [16–19]. Carbon-based electrodes are especially interesting since their surfaces can be covalently grafted by various molecules for versatile interface design.

Carbon tends to be more compatible with biological tissues than other commonly used electrode materials [19]. Among the carbon electrodes, carbon paste electrodes (CPE) are convenient conductive matrixes to prepare chemically modified electrodes (CMEs) by simple mixing of graphite/binder paste and modifier [20]. The CPEs can provide a suitable electrode substrate for preparation of modified electrodes.

Here, we report the preparation and application of a 2,2'-(1,3-propanediylbisnitrilo-ethylidene)bis-hydroquinone (PBNBH, Scheme 1) / TiO<sub>2</sub> nanoparticle modified carbon paste electrode (PBNBH-TNMCPE) as a new electrocatalyst for the electrocatalytic procedure and the determination of AA in an aqueous buffer solution. The analytical performance of the modified electrode was also evaluated for AA quantification in the presence of UA and FA.



**Scheme 1.** Structure of 2, 2'-(1, 3-propanediylbisnitrilo-ethylidene)-bis-hydroquinone

## 2. MATERIALS AND METHODS

### 2.1. Materials

The AA, UA and FA were purchased from Merck (Darmstadt, Germany). All other reagents used in this study were of analytical grade.

Graphite fine powder (Merck) and paraffin oil (DC 350, Merck, density = 0.88 g cm<sup>-3</sup>) were used as binding agents for the graphite pastes. The buffer solutions were prepared from ortho-phosphoric acid and its salts in the pH range from 2.0–11.0. The experimental results were obtained at room temperature.

### 2.2. Apparatus

A SAMA 500 electrochemical workstation (Sama Instruments, Iran) equipped with a personal computer was used for electrochemical measurements and data analysis. The SAMA software was used for control and data acquisition. A three-electrode electrochemical cell was employed. A PBNBH-TNMCPE, a saturated calomel electrode (SCE) and a platinum wire were used as the working, reference and auxiliary electrodes. All potentials are reported versus the SCE. A Metrohm 691 pH/ion meter was used for the pH measurements.

### 2.3. Typical procedure for preparation of 2, 2'-(1, 3-propanediylbisnitrilo-ethylidene)-bis hydroquinone

1,3-Diaminopropane (0.074 g, 1 mmol) was added in one portion to a mixture of 2,5-dihydroxyacetophenone (0.3 g, 2 mmol) in methanol and allowed to stir for 40 minutes. The progress of the reaction was monitored by thin layer chromatography (TLC). A yellow substance was precipitated, and the solid product was filtered off and washed with cold methanol. The obtained crude product was recrystallized in methanol and 2,2'-(1,3-propane-diybisnitrilo-ethylidene)-bis-hydroquinone was obtained as a yellow crystal with a melting point (m.p.) of 230-232°C and a 97% yield.

2,2'-(1, 3-propanediylbisnitrilo-ethylidene)-bis-hydroquinone; yellow solid; m.p: 230-232°C.

IR(KBr)/ $\nu$  ( $\text{cm}^{-1}$ ) 3100-3300 (br, OH), 3057, 2990, 2800, 1608(s, C=N), 1562, 1419, 1312, (s, Ar C=C), 1219 (s, C-O), 965, 840, 799 (s).

$^1\text{H}$  NMR (400 MHz/DMSO)/ $\delta$  ppm: 1.85 (m, 2 H,  $\text{CH}_2$ ), 2.1(s, 6 H, 2  $\text{CH}_3$ ), 3.44 (t, 4 H, 2  $\text{CH}_2$ ), 6.44 (d, 2 H, Ar), 6.56 (d of d, 2 H, Ar), 6.8 (d, 2 H, Ar), 8.4 (s, 2 H, OH), 15.2 (s, br, 2 H, OH).

$^{13}\text{C}$  NMR (100 MHz/DMSO)/ $\delta$  ppm: 16.1, 32.7, 48.4, 115.2, 119.53, 120.7, 121.6, 149.7, 157.0, 173.0.

#### 2.4. Preparation of electrode

The PBNBH (0.005 g) was dissolved in  $\text{CH}_3\text{Cl}$  and hand-mixed with 0.02 g of  $\text{TiO}_2$  nanoparticles and 0.0475 g of graphite powder with a mortar and pestle. The solvent was evaporated by stirring. Paraffin was added to the above mixture using a 4-mL syringe and mixed for 20 min until a uniformly wetted paste was obtained. The paste was then packed into the end of a glass tube (ca. 3.4 mm i.d. and 10-cm long). Electrical contact was made by pushing a copper wire down the glass tube into the back of the paste. When necessary, a new surface was obtained by pushing an excess of paste out of the tube and polishing it with a weighing paper.

### 3. RESULTS AND DISCUSSION

#### 3.1. Electrochemical behavior of PBNBH-TNMCPE

Previous studies on the electrochemical behavior of  $\text{TiO}_2$  nanoparticle-modified electrodes revealed that they can improve the kinetics of the electrode processes and the sensitivity of the measurements [21, 22]. These improvements are accompanied with a considerable decrease of the capacitive current, which causes the enhancement of the detection limit and resolution of adjacent waves in electroanalytical measurements.

Since the PBNBH complex is insoluble in aqueous solutions, it can be used in the carbon paste without leaching out from the electrode surface, which leads to a stable chemically modified electrode. The cyclic voltammogram of the PBNBH-TNMCPE exhibits an anodic peak during the forward scan, which is related to the oxidation of PBNBH to PBNBQ (its quinone form). Reduction of the quinone from PBNBQ to PBNBH occurs during the reverse scan (cathodic current peak). The peak separation potential,  $\Delta E_p = (E_{pa} - E_{pc})$ , was greater than the expected value (59 mV/n) for a reversible system. This suggests a quasi-reversible behavior in an aqueous medium.

In addition, the effect of the potential scan rate on the electrochemical properties of the PBNBH / PBNBQ redox couple in the PBNBH-TNMCPE was studied in an aqueous solution with cyclic voltammetry. Plots of the peak currents ( $I_p$ ) were linearly dependent on the scan rates from 50 to 400  $\text{mV s}^{-1}$ . A linear correlation was obtained between the peak current and the scan rate, indicating that the nature of the redox process was controlled in a diffusion-independent manner.

Laviron [23] derived general expressions for the linear potential sweep voltammetric response of surface-confined electroactive species with small enough concentrations:

$$E_{pa} = E^0 + A \ln [1 - \alpha/m] \quad (1)$$

and

$$E_{pc} = E^0 + B \ln [\alpha/m] \quad (2)$$

For

$$E_{pa} - E_{pc} = \Delta E_p > 200/n \text{ mV},$$

$$\log k_s = \alpha \log (1 - \alpha) + (1 - \alpha) \log \alpha - \log (RT/nFv) - \alpha (1 - \alpha) nF\Delta E_p / 2.3RT \quad (3)$$

where  $A = RT/(1 - \alpha)nF$ ,  $B = RT/\alpha nF$  and  $m = (RT/F) (k_s/\alpha n)$ .

From these expressions, it is possible to determine the transfer coefficient ( $\alpha$ ) by measuring the variation of the peak potentials with scan rate ( $v$ ) as well as the apparent charge transfer rate constant ( $k_s$ ) for the electron transfer between the electrode and the surface-confined material.

A plot of  $E_p$  as a function of  $\log v$  yields one straight line with a slope equal to  $2.3RT/(1 - \alpha)nF$  for the anodic peak. For scan rates above  $400 \text{ mVs}^{-1}$ , the values of  $E_{pa}$  were proportional to the logarithm of the scan rate, as indicated by Laviron. Using such a plot and Eq. (3), the values of  $\alpha$  and  $k_s$  were determined to be 0.34 and  $1.55 \text{ s}^{-1}$ , respectively.

The values for the surface concentration ( $\Gamma$ ) of the modified carbon paste electrode (MCPE), given in  $\text{mol cm}^{-2}$ , were obtained from the following equation [24]:

$$I_p = n^2 F^2 A \Gamma v / 4RT \quad (4)$$

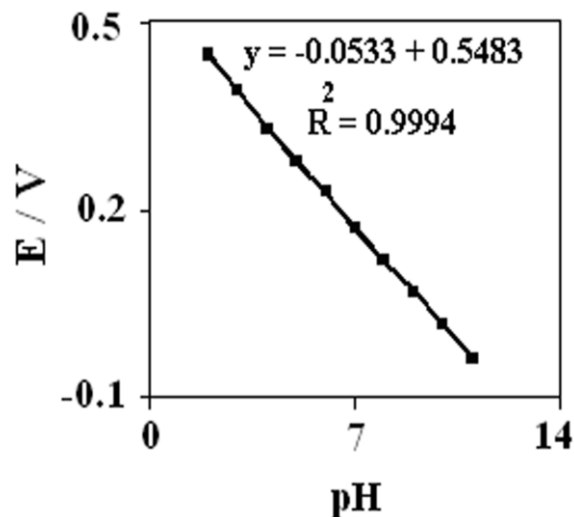
where  $n$  represents the number of electrons involved in the reaction,  $A$  is the surface area ( $\text{cm}^2$ ) of the MCPE,  $\Gamma$  ( $\text{mol cm}^{-2}$ ) is the surface coverage and other symbols have their usual meanings. From the slope of the anodic peak currents versus scan rate, the calculated surface concentration of PBNBH was  $2.9 \times 10^{-10} \text{ mol cm}^{-2}$  for  $n = 2$ .

### 3.2. Effect of pH on the electrochemical behaviors of the PBNBH-TNMCPE

The effect of the medium's pH on the electrochemical signal of the PBNBH-TNMCPE was investigated (Fig. 1). The pH of the solutions was adjusted using buffer solutions from pH 2.0–11.0. The peak potential changes over the pH range of 2.0–11.0, and there was a linear range, which can be described by the following equation:

$$E_p = -0.053 \text{ pH} + 0.5483 \quad R^2 = 0.9994 \quad (5)$$

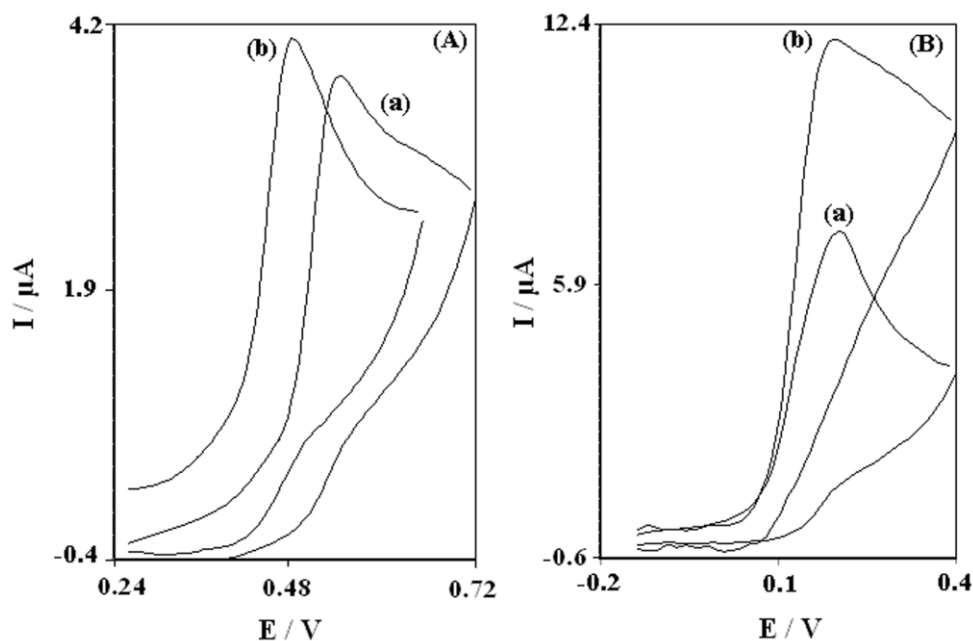
Such behavior suggests that it obeys the Nernst equation for a transfer reaction of two electrons and protons [25].



**Figure 1.** Dependence of PBNBH-TNMCPE anodic peak currents on the pH of the buffer solutions

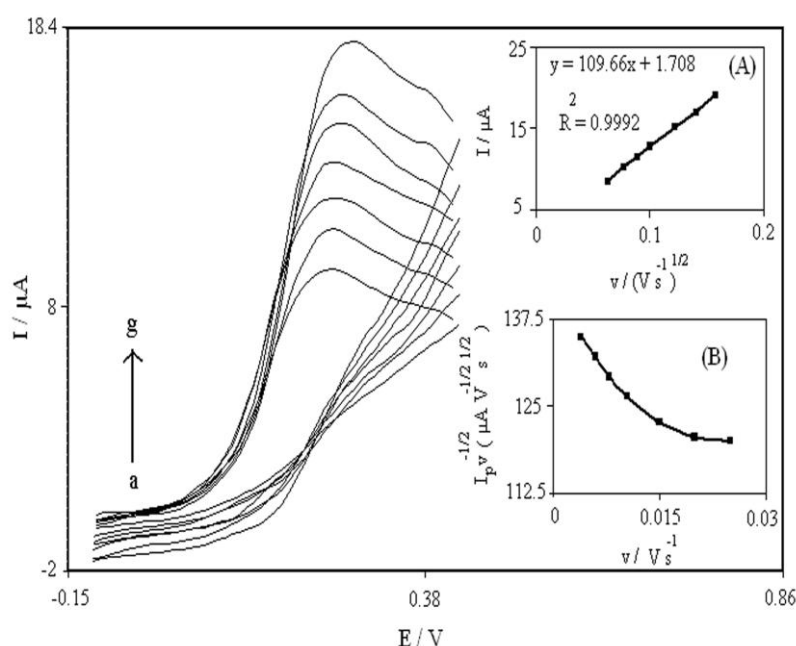
### 3.3. Electrocatalytic oxidation of AA at PBNBH-TNMCPE

Figure 2 depicts the cyclic voltammetric responses from the electrochemical oxidation of 0.3 mM AA at the bare CPE (Fig. 2A, curve a), TiO<sub>2</sub> nanoparticle-modified carbon paste electrode (TNMCPE) (Fig. 2A, curve b), PBNBH-modified carbon paste electrode (MCPE) (Fig. 2B, curve a) and PBNBH-TNMCPE (Fig. 2B, curve b).



**Figure 2.** A Cyclic voltammograms of 0.3 mM AA in a 0.1 M phosphate buffer solution (pH 7.0) at the (a) Bare-CPE and (b) TNMCPE. 2. B Cyclic voltammograms of 0.3 mM AA in 0.1 M phosphate buffer solution (pH 7.0) at the (a) PBNBH-MCPE and (b) PBNBH-TNMCPE. In all cases, the scan rate was 20 mV s<sup>-1</sup>

As shown, the anodic peak potential for AA oxidation at the PBNBH-MCPE (Fig. 2B, curve a) and PBNBH-TNMCPE (Fig. 2B, curve b) was about 180 mV, but was about 560 mV at the bare CPE (Fig. 2A, curve a). At the TNCPE (Fig. 2A, curve b), the peak potential was about 480 mV. Based on these results, we concluded that the best electrocatalytic effect for AA oxidation was at the PBNBH-TNMCPE (Fig. 2B, curve b). The peak potential of AA oxidation at the PBNBH-TNMCPE (Fig. 2B, curve b) shifted by about 300 and 380 mV toward negative values when compared with that at the TNCPE (Fig. 2A, curve b) and bare CPE (Fig. 2A, curve a), respectively. Similarly, when comparing the oxidation of AA at the PBNBH-MCPE (Fig. 2B, curve a) and PBNBH-TNMCPE (Fig. 2B, curve b), a dramatic enhancement of the anodic peak current at the PBNBH-TNMCPE (Fig. 2B, curve b) relative to that obtained at the PBNBH-MCPE (Fig. 2B, curve a) was observed. The data clearly show that the combination of TiO<sub>2</sub> nanoparticles and mediator (PBNBH) significantly improve the characteristics of AA oxidation.



**Figure 3.** Cyclic voltammograms of 0.5 mM AA at the PBNBH-TNMCPE at different scan rates in 0.1 M phosphate buffer solution (pH 7.0). (a-g: 4, 6, 8, 10, 15, 20 and 25 mV s<sup>-1</sup>, respectively). Insets: (A) Electrocatalytic current versus the square root of the scan rate (B). Scan rate-normalized current ( $I_p/v^{1/2}$ ) as a function of the scan rate

The results of electrocatalytic oxidation of AA at the surface of chemically modified electrodes by other mediators are given in Table 1 [26-30]. Compared with other electrodes, the proposed electrode exhibits a good electrocatalytic effect for AA oxidation.

To obtain information about the catalytic mechanism, cyclic voltammograms of an AA solution at different scan rates were recorded. Figure 3 shows the cyclic voltammograms of a PBNBH-TNMCPE at various scan rates obtained in a 0.1 M phosphate buffer solution (pH 7.0) containing 0.5 mM AA. The anodic oxidation current of AA is proportional to the square root of the scan rate (Fig.

3A), indicating that the reaction is controlled by AA diffusion at sufficiently positive potential according to following equation [25]:

$$I_p = 3.01 \times 10^5 n [(1-\alpha)n_a]^{1/2} A C_b D^{1/2} \nu^{1/2} \quad (6)$$

A plot of the sweep rate (Fig. 3B) normalized current ( $I_p/\nu^{1/2}$ ) versus sweep rate (4-25  $\text{mV s}^{-1}$ ) shows the characteristic shape of an EC' mechanism.

Andrieux and Savéant [31] have analyzed CVs in the framework of a model of redox chemically modified electrode. Based on extensive computations, a working curve showing the relationship between numerical values of the constant,  $I_{\text{cat}}/nFAC_b(DnF\nu/RT)^{1/2}$ , and  $\log[k_h/(DnF\nu/RT)^{1/2}]$  (Figure 1b. of Andrieux's article) was given, where  $D$  and  $C_b$  are the diffusion coefficient ( $\text{cm}^2 \text{s}^{-1}$ ) and bulk concentration ( $\text{mol cm}^{-3}$ ) of AA, respectively, and the other parameters have their usual meanings.

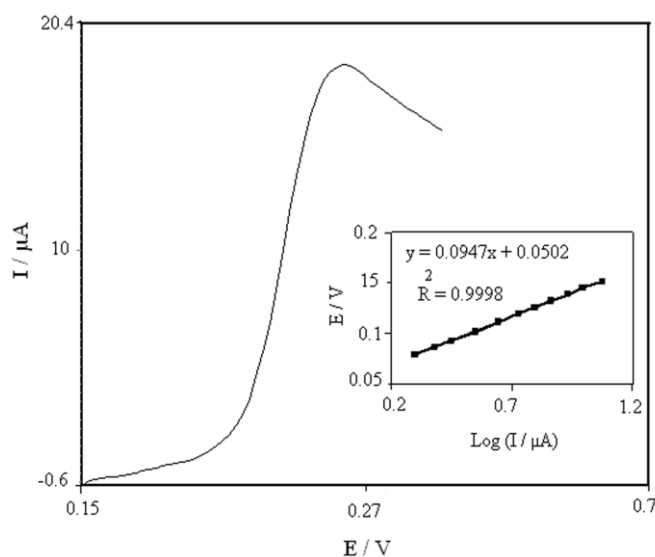


**Figure 4.** Linear sweep voltammogram of 0.5 mM AA at the PBNBH-TNMCPE in a 0.1 M phosphate buffer solution (pH 7.0). Inset shows the Tafel plot derived from the current-potential curve recorded at a scan rate of  $25 \text{ mV s}^{-1}$  and the dependence of the peak potential,  $E$ , on  $\log(I)$

The value of the catalytic reaction rate constant between AA and the PBNBH-TNMCPE ( $k_h$ ) can be calculated from such a working curve. For low scan rates ( $5\text{-}25 \text{ mVs}^{-1}$ ), at the PBNBH-TNMCPE, an analysis of the CVs yielded the average value for the ratio of  $I_{\text{cat}}/nFAC_b(DnF\nu/RT)^{1/2}$  to be 0.3, in the presence of 0.5 mM AA. Using this value and the theoretical paper by Andrieux and Saveant [31], the average value of  $k_h$  was found to be  $3.23 \times 10^{-3} \text{ cm s}^{-1}$  (for scan rates of 4, 6, and  $8 \text{ mV s}^{-1}$ ). This value of  $k_h$  helps to explain the sharp feature of the catalytic peak observed for the catalytic oxidation of AA at the PBNBH-TNMCPE.

Figure 4 shows linear sweep voltammograms of 0.5 mM AA in a 0.1 M phosphate buffer solution (pH 7.0). The inset of Fig. 4 shows a Tafel plot drawn from data of the rising part of the

current–voltage curve recorded at a scan rate of 25 mVs<sup>-1</sup>. This part of voltammogram, known as the Tafel region, is affected by electron transfer kinetics between the substrate (AA) and surface-confined PBNBH-TNMCPE, assuming the deprotonation of the substrate as a sufficiently fast step. In this condition, the number of electrons involved in the rate-determining step can be estimated from the slope of the Tafel plot. According to the Tafel slope equation and a slope of 0.0947 V decade<sup>-1</sup>, the charge transfer coefficient was calculated to be  $\alpha = 0.37$ .

### 3.4. Chronoamperometric studies

In chronoamperometry studies, the current,  $i$ , for the electrochemical reaction (at a mass-transport-limited rate) of an electroactive material (AA in this case) that diffuses to an electrode surface with a diffusion coefficient,  $D$ , is described by the Cottrell equation [25]:

$$I = nFAD^{1/2}C_b\pi^{-1/2}t^{-1/2} \quad (7)$$

where  $D$  is the diffusion coefficient,  $C_b$  is the bulk concentration of AA, and the other parameters have their usual meanings. Under diffusion (mass transport) control, a plot of  $i$  versus  $t^{-1/2}$  will be linear, and the value of  $D$  can be obtained from the slopes. We carried out such experiments on a PBNBH-TNMCPE by setting the potential at 0.3 V. The slopes of the resulting straight lines were then plotted versus the AA concentration; from the slope of this plot (46.105), the diffusion coefficient of AA was found to be  $1.9 \times 10^{-5} \text{ cm}^2 \text{ s}^{-1}$ .

### 3.5. Calibration plot and limit of detection

Since differential pulse voltammetry (DPV) has a much higher current sensitivity and better resolution than cyclic voltammetry, it was used to estimate the lower limit of AA detection. In addition, the charging current contribution to the background current, which is a limiting factor in the analytical determination, is negligible in DPV mode. Voltammograms clearly show that the plot of peak current versus AA concentration is composed of two linear segments with different slopes (slopes of  $0.785 \mu\text{A} \cdot \mu\text{M}^{-1}$  for the first linear segment and  $0.0702 \mu\text{A} \cdot \mu\text{M}^{-1}$  for the second linear segment), corresponding to two different ranges of substrate concentration ( $4.0\text{--}10.0 \mu\text{M}$  for the first linear segment and  $10.0\text{--}600.0 \mu\text{M}$  for the second linear segment). The decrease in sensitivity (slope) in the second linear range is likely due to kinetic limitations. The detection limit ( $2\sigma$ ) for AA in the lower range region was found to be  $0.4 \mu\text{M}$ . This value is comparable with values reported by other research groups (Table 1).

### 3.6. Simultaneously determination of AA, UA and FA

One of the main objectives of the present study was the development of a modified electrode capable of electro-catalytic oxidation of AA and separation of the electrochemical responses of AA, UA and FA.

The use of PBNBH-TNMCPE for the simultaneous determination of AA, UA and FA was demonstrated by simultaneously changing the concentrations of AA, UA and FA. The differential pulse voltammetric results show that the simultaneous determination of AA, UA and FA with three well-defined anodic peaks is possible at the modified electrode (Fig. 5). The linear dynamic ranges of UA and FA were 100.0-140.0 and 14.0-230.0  $\mu\text{M}$ , respectively.

**Table 1.** Comparison of the efficiency of modified electrodes used in the electrocatalysis of ascorbic acid

Substrate	Modifier	Method	pH and Peak potential / shift (mV)		Scan rate / (mV/s)	Detection limit (M)	Dynamic Range (M)	Reference
Platinum Electrode	Naphthol Green B	Voltammetry	4.5	320	50	$1.1 \times 10^{-4}$	$2.4 \times 10^{-4} - 2.5 \times 10^{-2}$	26
Glassy Carbon Electrode	Cobalt phthalocyanine nanoparticles	Potentiometry	7.0	190	200	$1.0 \times 10^{-7}$	$5.5 \times 10^{-7} - 1.0 \times 10^{-2}$	27
Carbon Paste Electrode	2,7-Bis(ferrocenyl ethyl)fluoren-9-one	Voltammetry	7.0	300	10	$9.0 \times 10^{-6}$	$3.1 \times 10^{-5} - 3.3 \times 10^{-3}$	28
Gold Electrode	Ferrocene	Voltammetry	5.8	–	50	$2.0 \times 10^{-7}$	$1.0 \times 10^{-6} - 5.0 \times 10^{-4}$	29
Glassy Carbon Electrode	Ruthenium oxide	Voltammetry	5.0	250	100	$8.0 \times 10^{-5}$	$8.8 \times 10^{-5} - 2.32 \times 10^{-3}$	30
Carbon Paste Electrode and TiO <sub>2</sub> Nanoparticles	2,2'-(1,3propane diylbisnitriloethylidene)-bis hydroquinone	Voltammetry	7.0	380	25	$3.8 \times 10^{-7}$	$4.0 \times 10^{-6} - 6.0 \times 10^{-4}$	This work

The sensitivities of the modified electrode towards the oxidation of AA, UA and FA were found to be  $0.80 \mu\text{A}\mu\text{M}^{-1}$  (Inset A of Fig. 6),  $0.085 \mu\text{A}\mu\text{M}^{-1}$  (Inset B of Fig. 6) and  $0.051 \mu\text{A}\mu\text{M}^{-1}$  (Inset C of Fig. 6), respectively, whereas the sensitivities towards AA in the absence and presence of UA and were found to be 0.78 (absence of UA and FA) and 0.8 (presence of UA and FA)  $\mu\text{A}\mu\text{M}^{-1}$ . These results indicate that the oxidation processes of AA, UA and FA at the PBNBH-TNMCPE are independent and therefore simultaneous measurements of the three analytes are possible without any

interference. If the AA signal had been affected by the UA and FA signals, the above-mentioned slopes would be different.

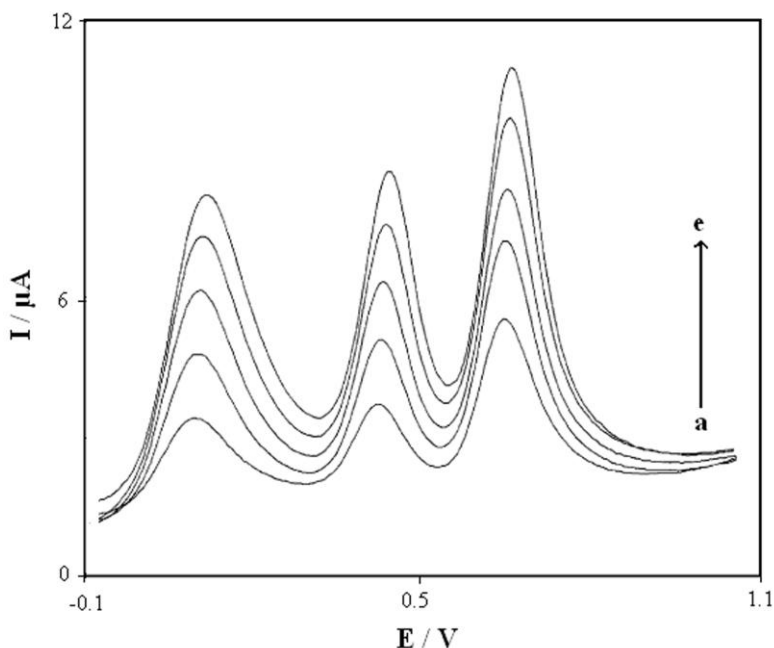


**Figure 5.** (A) Differential pulse voltammograms of the PBNBH-TNMCPE in a 0.1 M phosphate buffer solution (pH 7.0) in mixed solutions of (a-e: 4.0, 6.0, 8.0 and 10.0  $\mu\text{M}$  AA; 100.0, 110.0, 120.0, 130.0, and 140.0  $\mu\text{M}$  UA; and 140.0, 160.0, 180.0, 210.0, and 230.0  $\mu\text{M}$  FA) with potential scan rates of  $25 \text{ mV s}^{-1}$

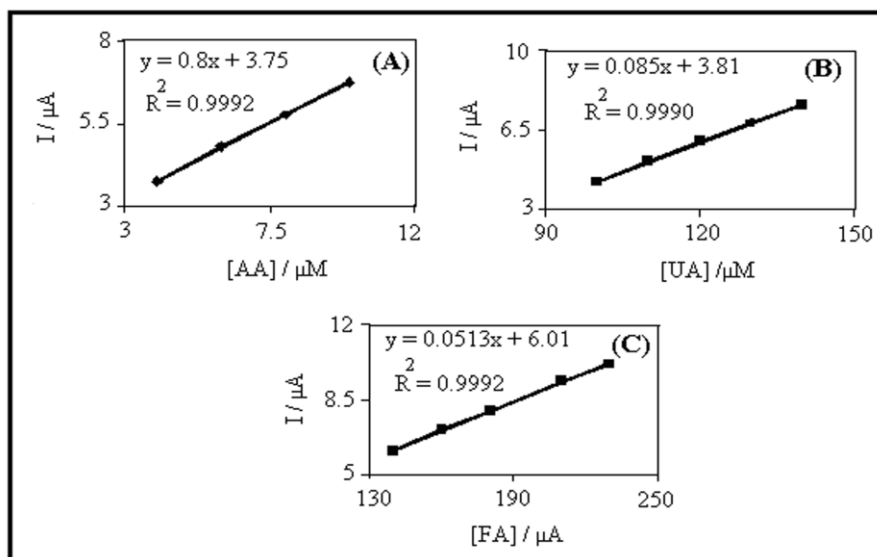


**Figure 6.** Plots of the peak current as a function of the concentration of: (A) 4.0, 6.0, 8.0, 10.0, and 20.0  $\mu\text{M}$  AA (B) 100.0, 110.0, 120.0, 130.0, and 140.0  $\mu\text{M}$  UA (C) with concentrations of 140.0, 160.0, 180.0, 210.0, and 230.0  $\mu\text{M}$  FA in a 0.1 M phosphate buffer solution (pH 7.0) at the PBNBH-TNMCPE.

### 3.7. Determination of AA in real samples

The proposed PBNBH-TNMCPE was found to work well under laboratory conditions. The electrode was also successfully applied to the direct determination of AA content of pharmaceutical samples. The AA content in pharmaceutical samples was determined by the standard addition method to prevent any matrix effect. The results for the analysis of pharmaceutical samples with the voltammetric method compared favorably with those obtained by the USP standard method (Table 2).

**Table 2.** Determination of ascorbic acid in real samples

Pharmaceutical preparation	Proposed method (mg) (%RSD)	Iodine method (mg) (%RSD)
Ampoule	479.5 (3.0)	475.3 (3.0)
Multivitamin syrup	54.6 (1.8)	51.8 (2.1)

## 4. CONCLUSIONS

The electrochemical behavior of 2,2'-(1,3-propanediylbisnitrilo-ethylidene)bis-hydroquinone / TiO<sub>2</sub> nanoparticles was studied. Oxidation of AA is catalyzed at pH 7.0, whereas the peak potential of AA is shifted by 380 and 80 mV to a less positive potential at the surface of the PBNBH-TNMCPE and TNMCPE, respectively. The catalytic peak currents obtained from DPV were linearly dependent on the AA concentration in the range of 4.0-600.0  $\mu$ M. The detection limit ( $2\sigma$ ) for AA was 0.4  $\mu$ M with a correlation coefficient of 0.9998. The results show that UA and FA have no interference with AA detection, and therefore UA, FA, and AA can be simultaneously detected. The proposed method can also be applied to the determination of AA in pharmaceutical samples.

## ACKNOWLEDGEMENTS

The authors wish to thank the Yazd University Research Council and the IUT Research Council and Excellence in Sensors for financial support of this research. We gratefully acknowledge Dr N. Taghavinia of Sharif University of Technology for preparing of the nanoparticles.

## References

1. B. O'Regan, M. Gratzel, *Nature*, 353 (1991) 737-740.
2. A.Eychmuller, *J. Phys. Chem. B* 104 (2000) 6514-6528.
3. J.N. Clifford, E. Palomares, M.K. Nazeeruddin, R. Thampi, M. Gratzel, *J. Am. Chem. Soc.* 126 (2004) 5670-5671 and J. Solla-Gullon, V. Monteil, A. Aldaz and J. Clavillier, *Journal of Electrochemical Society*, 150 (2003) 1-10.

4. C.J. Tavares, J. Vieira, L. Rebouta, G. Hungerford, P. Coutinho, V. Teixeira, J.O. Carneiro, A.J. Fernandes, *Mater. Sci. Eng. B*, 138 (2007) 139-143.
5. E. Topoglidis, A.E.G. Cass, G. Gilardi, S. Sadeghi, N. Beaumont, J. R. Durrant, *Anal. Chem.* 70 (1998) 5111-5113.
6. D. Beydoun, R. Amal, *Mater. Sci. Eng. B*, 94 (2002) 71-81.
7. C.A.B. Clemetson, *Vitamin C*, CRC Press, Boca Raton, FL, 1989.
8. D.W. Martin, P.A. Jr, V.W. Mayes, E. Rodwell, S. Harper, *Review of Biochemistry*, 19th ed., Lange Medical Publications, Los Altos, CA, 1983.
9. G. Dryhurst, K.M. Kadish, F. Scheller, R. Renneberg, *Biological Electrochemistry* vol 1, Academic Press, New York, 1982.
10. V.V.S. Eswara, H.A. Mottola, *Anal. Chem.* 46 (1974) 1777-1781.
11. H.A. Harper, *Review of Physiological Chemistry*, 13th ed., Lange Medical Publications, Los Altos, CA, 1977.
12. J. Zheng, X. Zhou, *Bioelectrochemistry*, 70 (2007) 408-415.
13. J. Zheng, *General Biochemistry (in Chinese)*. High Education Press of China, Beijing 1985.
14. M. Mazloun-Ardakani, M. A. Karimi, M. M. Zare, S. M. Mirdehghan, *Int. J. Electrochem. Sci.* 3 (2008) 246.
15. M. Mazloun-Ardakani, Z. Taleat, *Int. J. Electrochem. Sci.* 4 (2009) 694.
16. M. Mazloun Ardakani, Z. Taleat, H. Beitollahi, M. Salavati-Niasari, B.B.F. Mirjalili, N. Taghavinia, *J. Electroanal. Chem.* 624 (2008) 73-78.
17. M. Mazloun-Ardakani, F. Habibollahi, H. R. Zare, H. Naeimi, *Int. J. Electrochem. Sci.* 3 (2008) 1236.
18. H. Beitollahi, M. Mazloun Ardakani, B. Ganjipour, H. Naeimi, *Biosens. Bioelectron.* 24 (2008) 362-368.
19. Y. Liu, Q.J. Song, L. Wang, *Microchem. J.*, 91 (2009) 222-226.
20. M. Mazloun-Ardakani, F. Habibollahi, H. R. Zare, H. Naeimi, M. Nejati, *J. Applied Electrochem.* 39 (2009) 1117-1124.
21. W.M. Liu, Y. Chen, G.T. Kou, T Xu, D C Sun., *Wear* 254 (2003) 994-1000.
22. S. Yuan, W. Chen, S. Hu, *Mat. Sci. Engin.* 25 (2005) 479-485.
23. E. Laviron, *J. Electroanal. Chem.* 101 (1979) 19-28.
24. M. Sharp, M. Petersson, K. Edstrom, *J. Electroanal. Chem.* 95 (1979) 123-130.
25. A.J. Bard, L.R. Faulkner, *Electrochemical methods. Fundamentals and applications*, 2nd ed., Wiley, New York, 2001.
26. A. Mohadesi, M.A. Taher, *Sens. Actuators B* 123 (2007) 733-739.
27. K. Wang, J. Xu, K. Tang, H. Chen, *Talanta* 67 (2005) 798-805.
28. J.B. Raouf, R. Ojani, H. Beitollahi, R. Hosseinzadeh, *Electroanalysis*, 18 (2006) 1193-1201.
29. S. Wang, D. Du., *Sens. Actuators B* 97 (2004) 373-378.
30. P. Shakkthivel, S.M. Chen, *Biosens. Bioelectron.* 22 (2007) 1680-1687.
31. C.P. Andrieux, J. Savéant, *J. Electroanal. Chem.* 93 (1978) 163-168.